Metabolic Brain Disease (2022) 37:2261–2275
https://doi.org/10.1007/s11011-022-01019-z

ORIGINAL ARTICLE

Schisandra chinensis (Turcz.) Baill. essential oil exhibits antidepressant-like effects and against brain oxidative stress through Nrf2/HO-1 pathway activation

Liang Tan[1] · Yunfang Yang[2] · Jing Peng[2] · Yue Zhang[2] · Bo Wu[2] · Bosai He[2] · Ying Jia[2] · Tingxu Yan[2]

Received: 19 April 2022 / Accepted: 26 May 2022 / Published online: 6 June 2022

Abstract

The present study aimed to evaluate the antidepressant-like effect of essential oils from *Schisandra chinensis* (Turcz.) Baill. (SEO) and its possible mechanisms of SEO. The behavioral despair mouse model in vivo and H_2O_2-induced PC12 cells model in vitro were employed. And the potential effective components were identified by the spectrum-effect relationships analysis. SEO significantly decreased the immobility time in the forced swimming test and tail suspension test, which indicated a promising antidepressant-like effect of SEO in depressed mice. The decreased levels of SOD, GSH, and CAT, and increased levels of MDA were significantly reversed by SEO treatment, which showed good antioxidant activities both in vitro and in vivo. Besides, SEO significantly promoted the nuclear translocation of Nrf2 and the expression of HO-1 in depressed mice and H_2O_2-induced PC12 cells. The histopathological examination results showed a potential neuronal protective effect of SEO in the hippocampus and cortex. Furthermore, the upregulation of PI3K/AKT/GSK3β signaling was observed after SEO treatment in the H_2O_2-induced PC12 cells. Additionally, based on the spectrum-effect relationship analysis, 9 peaks were identified as positively correlated with the antioxidant activity of SEO. These results suggested that SEO promoted Nrf2/HO-1 pathway to improve the oxidative stress status and exerted the antidepressant-like effects.

Keywords *Schisandra chinensis* (Turcz.) Baill. · Depression · Spectrum-effect relationships · Antioxidant activity · Nrf2/HO-1 signaling · PI3K/AKT/GSK3β signaling

Introduction

Major depressive disorder (MDD) is one of the most disabling disorders causing a great burden globally on patients and societies. Especially, the COVID-19 pandemic worldwide is concerning, it has affected depressive patients' physical and mental health fundamentally due to social isolation and lack of care. However, the pathogenesis of MDD remains unclear, oxidative stress, neuroinflammation, gut microbiome disorder, and HPA axis dysfunction can induce the occurrence of depression. The available treatment for depression is still insufficient since 30% of patients are treatment-resistant. Thus, there is an urgent need to find new antidepressants to treat depression.

Traditional Chinese medicine (TCM) has been widely used to treat mood disorders for many years in China. According to TCM theory, herbs systematically alter the physiological functions of the whole body and improve depressive symptoms gradually. Essential oils (EOs) are the main components of TCM with promising pharmacological activities, such as anti-oxidant, anti-bacterial, anti-cancer, and anti-allergic effects. In addition, EOs also have great potential effects on depression, insomnia, and neuronal injury due to the high hydrophobicity which can make EOs are easier to pass through the blood-brain barrier (BBB) and play positive roles in the central nervous system (CNS) disease treatment (Zhang et al. 2021b). However, EOs contain multicomponent which can aim at multiple targets in vivo, so it is difficult to identify the active compounds. Spectrum-effect relationships study has been widely used to screen the effective components in TCM. The fingerprint spectrum is

✉ Tingxu Yan
ytxsyphu@163.com

[1] Qinghai Key Laboratory of Qinghai-Tibet Plateau Biological Resource, Northwest Institute of Plateau Biology, Chinese Academy of Sciences, Xining 810001, China

[2] School of Functional Food and Wine, Shenyang Pharmaceutical University, Wenhua Road 103, Shenyang 110016, China

usually obtained by using the GC-MS method. The correlation between the fingerprint spectrum and bioactivity of EOs could locate the possible bioactivity-related chemicals. In this study, the spectrum-effect relationship analysis was applied to identify the components with the anti-oxidant effect of EOs.

Schisandra chinensis (Turcz.) Baill. (SCH) is mainly distributed in East Asia, including China, Russia, and Japan, and has long been used to treat hepatitis, insomnia, and convulsions. Moreover, our lab previously found that lignans of SCH showed good antidepressant-like effects on different depressed animal models. Recent studies reported that EOs of SCH exhibited inhibitory activity on ROS production which could be used as an excellent anti-oxidant (Lee et al. 2021). Therefore, we intend to investigate the antidepressant-like effect of EOs of SCH and explore the detailed anti-oxidant mechanism and identify the components with antidepressant-like effect by the spectrum-effect relationship analysis in the present study.

Materials and methods

Chemicals and reagents

DPPH and ABTS were purchased from Dalian Meilunbio Institute (Dalian, China). ELISA kits used for the determination of MDA, SOD, CAT, and GSH were obtained from Nanjing Jiancheng Bioengineering Institute (Nanjing, China). All other reagents were of analytical grade.

SEO extraction

The fruits of *S. Chinensis* were purchased from trading companies in China and identified by Professor Ying Jia (Department of Pharmacognosy, Shenyang Pharmaceutical University) according to the guidelines of the Chinese Pharmacopoeia (2020). SEO was obtained using the hydrodistillation system-Clevenger type apparatus. The detailed procedure is as in our previous report (Yan et al. 2021). The SEO was dried over Na_2SO_4 and stored at 4 °C until further analysis.

Animals and treatment

Adult male C57BL/6 mice (20 ± 2 g) were obtained from the animal center of Shenyang Pharmaceutical University. All mice were allowed to habituate to the novel environment for 1 week prior to the experiment with food and water available ad libitum. All experiments were approved by the animal care committee of Shenyang Pharmaceutical University and performed in compliance with the national institutes of health and institutional guidelines for the humane care of animals. The mice were randomly divided into 4 groups (10 mice/group): Vehicle group, Fluoxetine (Flu) group (15 mg/kg, *i.g.*), SEO 250 group (250 mg/kg, *i.g.*) and SEO 750 group (750 mg/kg, *i.g.*). Flu and SEO were suspended in 0.5% sodium carboxymethylcellulose (CMC-Na), respectively. For the Vehicle group, the animals were given the same amount of 0.5% CMC-Na. The repeated drug treatment was performed once daily and continuously for 9 days.

Forced swimming test (FST)

FST was conducted according to the methods described previously (Armario 2021). In brief, the immobility time of each mouse was detected during the last 4 min of a single 6-min forced swim session.

Tail suspension test (TST)

TST was conducted as described previously with slight modifications (Zhang et al. 2021a). In brief, the immobility time of each mouse was recorded for the last 4 min following 2 min habituation during a 6 min test period.

ELISA assay

After the behavioral tests, the blood was collected and the supernatant was centrifuged at 4000 r/min for 15 min and stored at −80 °C with a rapidly stripped hippocampus and cortex for subsequent assays. The levels of MDA, SOD, CAT, and GSH in serum, liver, brain, and cell supernatant were detected using ELISA kits according to the manufacturer's protocol.

Western blot

The hippocampus, cortex, and cell supernatant were processed following the western blot procedure (Zhang et al. 2021c). The primary antibodies used in the present study including Nrf2 (Abcam, 1:1000), HO-1 (Abcam, 1:1000), PI3K (CST, 1:1000), p-PI3K (phosphor Y607) (CST, 1:1000), AKT (CST, 1:1000), p-AKT (phosphor Ser 473) (CST, 1:1000), GSK3β (CST, 1:1000), p-GSK3β (phosphor Ser 9) (CST, 1:1000), Lamin B (Proteintech, 1:1000) and β-actin (CST, 1:1000). Anti-rabbit IgG (CST, 1:2000) was used as the secondary antibody. The relative densities were detected using Image-Pro plus 6.0 analysis software.

Histopathological examination

After the behavioral tests, mice brains were removed immediately and fixed in formaldehyde solution, and then stained with hematoxylin and eosin after being cut in the coronal

plane. The slices of the hippocampus and cortex were examined under light microscopy.

Drug treatment and cell viability

PC12 cells were cultured in RPMI-1640 with 10% fetal calf serum at 37 °C in an incubator supplemented with 5% CO_2. Then, the cells were seeded and pre-incubated with various concentrations of SEO for 24 h, followed by the treatment of 300 μmol/L H_2O_2 for a further 24 h incubation. Subsequently, 20 μL MTT solution was added, followed by the MTT assay protocol. The experimental groups were as follow: Control, Vehicle (300 μmol/L H_2O_2), SEO (0.78–25 μg/mL + 300 μmol/L H_2O_2). SEO and H_2O_2 were dissolved in DMSO to certain concentrations, and the concentrations were selected by our preliminary experiments, and data was not shown. Fluoxetine (15 μmol/L) served as positive control drug as previously reported (Han and Lee 2009; Park et al. 2021).

Immunofluorescence assay

Transfected PC12 cell slides were deparaffinized and permeabilized with PBS/0.1% Triton X100 as described previously (Liu et al. 2021b). Slides were then incubated with anti-Nrf2 overnight at 4 °C, washed 3 times in PBS, then incubated with secondary antibody at 37 °C for 1 h. Cell nuclei were counterstained with DAPI/Fluorescence quenching agent (Beyotime). Stained cells were observed using a Leica fluorescence microscope.

GC-MS analysis

18 batches of SEO (Table 1) were analyzed by a GC-MS, and the analyses were carried out on devices Agilent 7000C equipped with an HP-5MS capillary column (30 m × 0.25 mm × 0.25 μm). In brief, the injector and detector temperatures were set as 230 °C and 230 °C, respectively. 1.0 μL of the sample was injected using split mode (split ratio 1:50). Helium was used as a carrier gas (1.2 mL/min). The column temperature was programmed as follows: the initial temperature was 60 °C for 2 min, then increased to 110 °C at 5 °C/min and maintained for 10 min, increased to 120 °C at 2 °C/min and maintained for 7 min, and finally increased to 180 °C at 5 °C/min for last 2 min. The total time for analysis was 47 min. The MSD (EI mode) was operated at 70 eV, and the scan range was set to 30–500 amu. Constituents were identified by comparison of their retention indices with those reported in the published literature. Further identification was made by comparison of the mass spectra with those listed in the NIST 2014 MS library. Relative concentrations of components were calculated by the area normalization method.

Table 1 Origins of SEO

No.	Origin	Essential oil Contents	The fingerprint ID
1	Jinzhou 1, Liaoning	1.03%	S1
2	Jinzhou 2, Liaoning	0.93%	S2
3	Huanren, Liaoning	1.34%	S3
4	Fushun 1, Liaoning	0.74%	S4
5	Fushun 2, Liaoning	0.58%	S5
6	Dandong 1, Liaoning	1.08%	S6
7	Dandong 2, Liaoning	1.13%	S7
8	Benxin 1, Liaoning	1.18%	S8
9	Benxi 2, Liaoning	0.92%	S9
10	Panjin, Liaoning	0.91%	S10
11	Donggang, Liaoning	0.94%	S11
12	Yingkou, Liaoning	1.07%	S12
13	Xinbin, Liaoning	0.98%	S13
14	Liaoyang 1, Liaoning	1.03%	S14
15	Liaoyang 2, Liaoning	0.95%	S15
16	Shenyang 1, Liaoning	0.81%	S16
17	Shenyang 2, Liaoning	1.16%	S17
18	Fuxin, Liaoning	0.93%	S18

DPPH assay

DPPH radical scavenging activity of samples was detected as described previously with some modifications (Wang et al. 2021b). Briefly, 2 mL of 0.2 mM DPPH was added to 0.2 mL of various concentrations (2–14 mg/mL) SEO solution. The mixture was shaken vigorously and left to stand for 30 min in the dark, and the absorbance was then measured at 517 nm. The assay was performed in triplicate. Ascorbic acid at the same concentrations was used as a reference. The radical scavenging activity was calculated by the following formula:

$$\text{Scavenging activity } (\%) = \left[1 - \left(A_1 - A_2\right)\right]/A_0 \times 100\%$$

Where A_0 is the absorbance of the control, A_1 is the absorbance in the presence of the extract, and A_2 is the absorbance of the sample only. The IC_{50} value represented the concentration of the compounds that caused 50% inhibition of DPPH radical formation.

ABTS assay

The ability to scavenge the ABTS radical cation ($ABTS^+$) was determined according to the previously reported method (Ong et al. 2021). The $ABTS^+$ solution was prepared by the reaction of 7 mM ABTS (10 mL) and 2.45 mM (10 mL) potassium persulphate after incubation at room temperature

in the dark for 16 h. It was then diluted with 80% ethanol to give an absorbance value of 0.700 ± 0.005 at 734 nm. The $ABTS^+$ solution (5 mL) was thoroughly mixed with the test samples at various concentrations (0.1 mL). The reaction mixture was allowed to stand at 30 °C for 30 min, and the absorbance at 734 nm was immediately recorded. Ascorbic acid at the same concentrations was used as a reference. The level of radical scavenging was calculated using the aforementioned equation for DPPH.

Spectrum-effect relationship analysis

To investigate the anti-oxidative stress effects of SEO, the partial least-squares regression (PLS) method was employed. The areas of common peaks of each fingerprint were set as the independent variables X, and the IC50 values of DPPH and ABTS were set as Y. If the regression coefficient of one peak was larger than zero, then it contained antioxidant components as previously reported (Zhang et al. 2018).

Statistical analysis

All data were analyzed with Analysis of Variance (ANOVA) using GraphPad Prism and descriptively expressed as mean ± SEM analyzed. $p < 0.05$ was considered statistically significant.

Results

Effects of SEO on the immobility time in TST and FST

The data of TST (Table 2) and FST (Table 3) both showed that SEO 250 and SEO 750 could significantly reduce the immobility time compared to the Vehicle group. SEO showed a promising antidepressant-like effect in depressed mice.

Table 2 Effect of SEO on the immobility time in the tail suspension test

Group	Dose (mg/kg)	Immobility time (s)
Vehicle	–	101.50 ± 10.45
Flu	15	67.83 ± 8.42***
SEO 250	250	84.83 ± 8.33*
SEO 750	750	55.33 ± 5.89***

The values represent the mean ± SEM (n = 10 in each group), *$p < 0.05$, ***$p < 0.001$ compared with the Vehicle group

Table 3 Effect of SEO on the immobility time in the forced swimming test

Group	Dose (mg/kg)	Immobility time (s)
Vehicle	–	124.67 ± 12.60
Flu	15	77.80 ± 10.76***
SEO 250	250	98.80 ± 11.56**
SEO 750	750	83.25 ± 6.45***

The values represent the mean ± SEM (n = 10 in each group), **$p < 0.01$, ***$p < 0.001$ compared with the Vehicle group

Effects of SEO on levels of SOD, MDA, CAT, and GSH in depressed mice

Figure 1 showed the levels of SOD, MDA, CAT, and GSH in the hippocampus, cortex, and serum. SEO 750 could significantly increase the levels of SOD, GSH, and CAT in the hippocampus, cortex, and serum, and reduce the levels of MDA in the hippocampus, cortex, and serum. These results indicated that SEO could effectively alleviate oxidative stress in depressed mice.

Effects of SEO on the expressions of Nrf2 in depressed mice

After FST and TST, expressions of nuclear Nrf2 in the hippocampus and cortex were significantly decreased. SEO treatment could significantly reverse these changes (Fig. 2), which illustrated that SEO might promote Nrf2 translocation to reduce oxidative stress.

Effects of SEO on histopathological changes in hippocampus and cortex

The neuronal integrity and orderliness of the hippocampus and cortex were detected by HE staining. In the Vehicle group, neurons in the hippocampus (DG and CA1 sections) and cortex were sparsely arranged, and the nuclei were deeply stained as well as condensed. SEO treatments significantly reversed neuronal loss and injury, the neurons in DG, CA1, and cortex were arranged neatly in rows, oval or round, rarely depigmented, and the nuclei were clearly visible (Fig. 3).

Fig. 1 The activities of SOD (**A**), GSH (**B**), CAT (**C**) and the levels of MDA (**D**) in hippocampus(1), cerebral cortex(2) and plasma(3). The values represent the mean ± SEM (n = 8 in each group), *$p < 0.05$, **$p < 0.01$, ***$p < 0.001$ compared with the Vehicle group

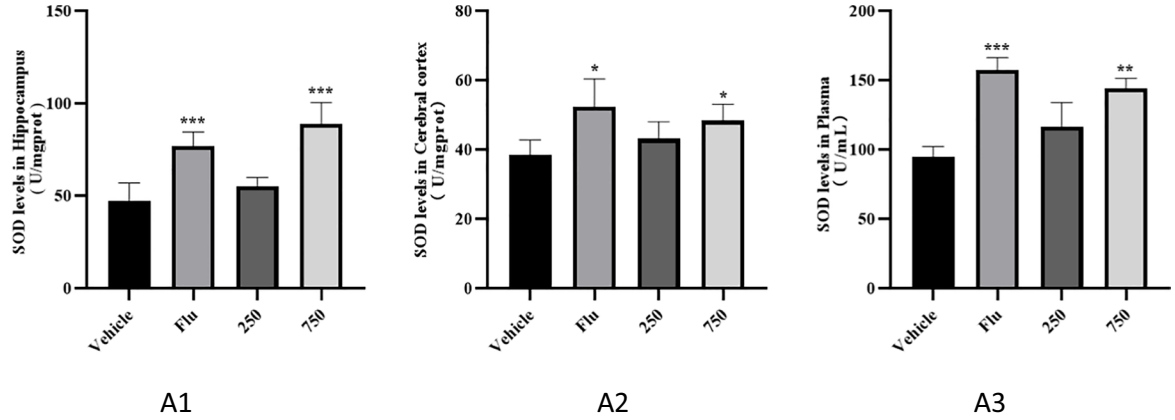

A1 A2 A3

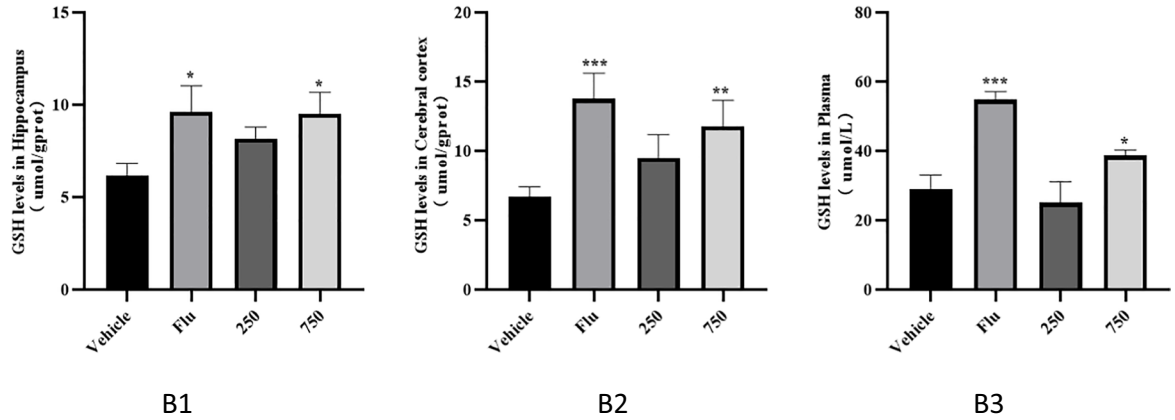

B1 B2 B3

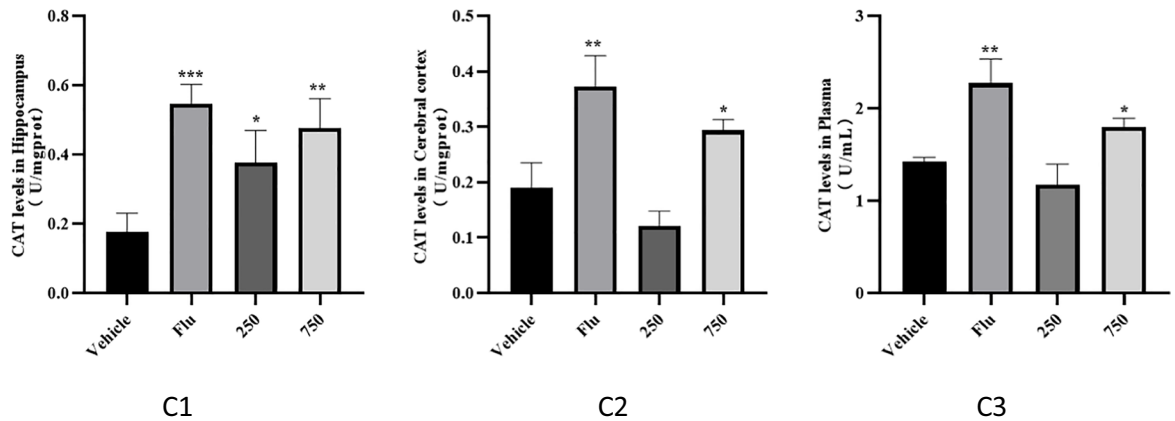

C1 C2 C3

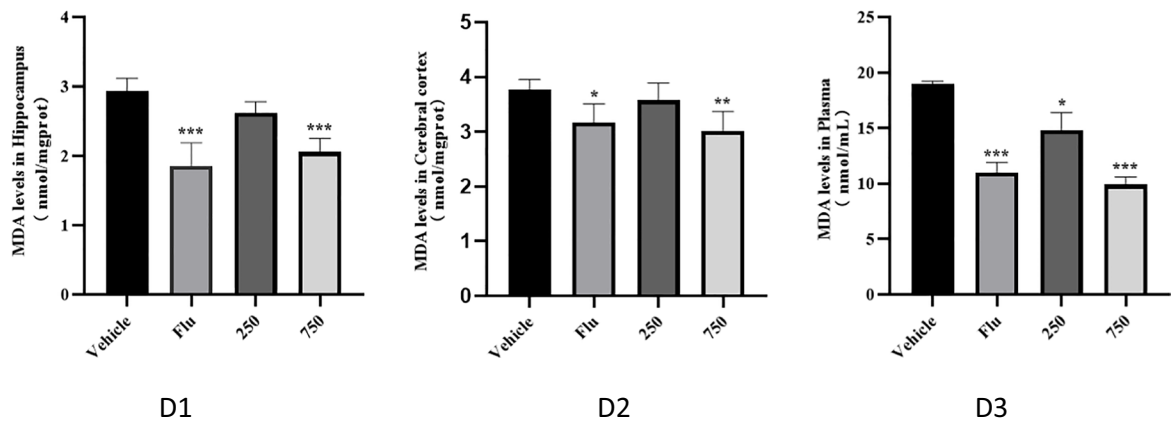

D1 D2 D3

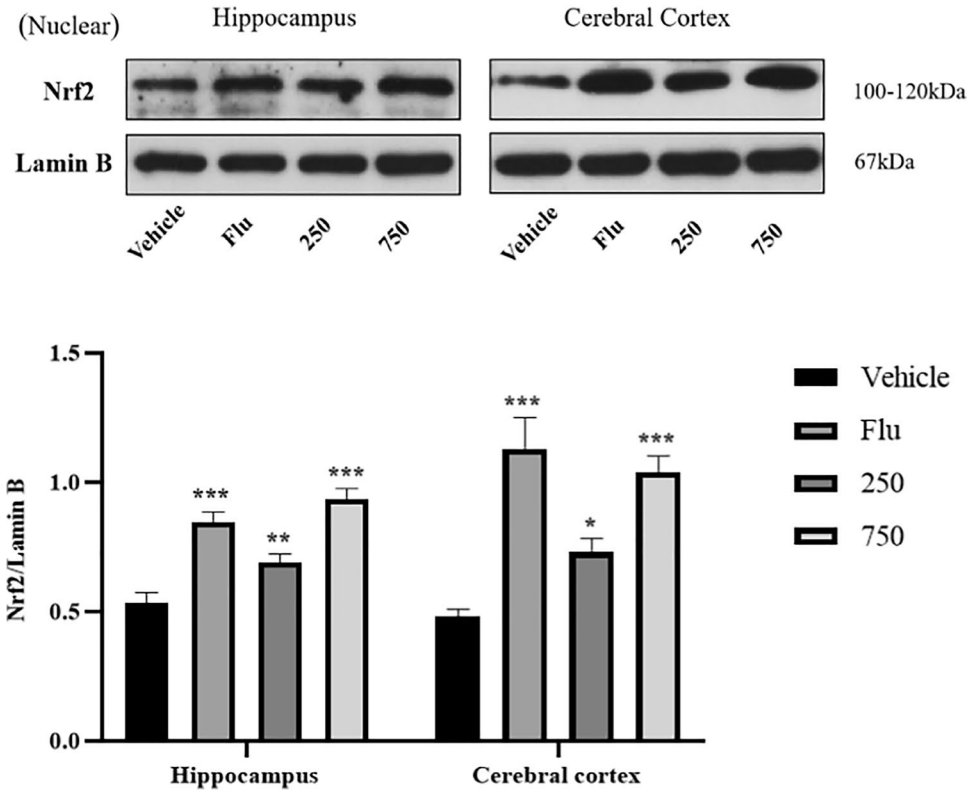

Fig. 2 The Effect of SEO on nuclear of Nrf2 expression in mice. (A) The expression of nuclear Nrf2 was detected by Western Blot using specific antibodies in mice. (**B**) graphs represented the arbitary density of blot signal. The values represent the mean ± SEM (n = 3 in each group), $^{*}p < 0.05$, $^{**}p < 0.01$, $^{***}p < 0.001$ compared with the Vehicle group

Effects of SEO on cell viability in H_2O_2-induced PC12 cells

MTT results showed in Fig. 4.Cell viability significantly decreased after H_2O_2 exposure, and SEO (1.56, 3.125, 6.25, 12.5, and 25 μg/mL) significantly increased the cell viability that indicating that SEO could effectively inhibit the oxidative stress caused by H_2O_2.

Effects of SEO on levels of SOD, GSH, CAT, and MDA in H_2O_2-induced PC12 cells

H_2O_2 induced significant decreases in levels of SOD (Fig. 5A), GSH (Fig. 5B), and CAT (Fig. 5C), and increases in levels of MDA (Fig. 5D). However, SEO (6.25 μg/mL) treatment dramatically increased the levels of SOD, GSH, and CAT, and reduced the levels of MDA.

Effects of SEO on Nrf2/HO-1 signaling in H_2O_2-induced PC12 cells

Figure 6A showed that SEO significantly promoted the Nrf2 translocation compared with the Vehicle group. Besides, the expression of HO-1 was significantly reduced by H_2O_2 treatment (Fig. 6B), and SEO could significantly increase the expression of HO-1, which indicated that the effects of anti-oxidative stress of SEO might be via the upregulation of Nrf2/HO-1 signaling.

Effects of SEO on PI3K/AKT/GSK3β signaling in H_2O_2-induced PC12 cells

As shown in Fig. 7, the ratios of p-PI3K/PI3K, p-AKT/AKT, and p-GSK3β/GSK3β were significantly reduced by H_2O_2 exposure, and SEO treatments significantly increased these ratios. These results suggested that PI3K/AKT/GSK3β signaling might be involved in the mechanism of anti-oxidative stress effects of SEO in H_2O_2-induced PC12 cells.

In vitro antioxidant activities

The DPPH radical scavenging activities of different batches of SEO are presented in Table 4. The IC50 value of the DPPH radical inhibitory concentrations of the 18 batches of SEO ranged from 2.99–8.24 mg/mL. S5 showed the weakest DPPH radical inhibitory capacity, and S6 showed the strongest capacity. The results of ABTS radical scavenging

Fig. 3 The histopathological changes in the Hippocampus and Cortex ▶ of Vehicle group (**A**), Flu group (**B**), 250 group (**C**), 750 group (**D**). The magnification was 200×. The arrow points to nuclear retraction

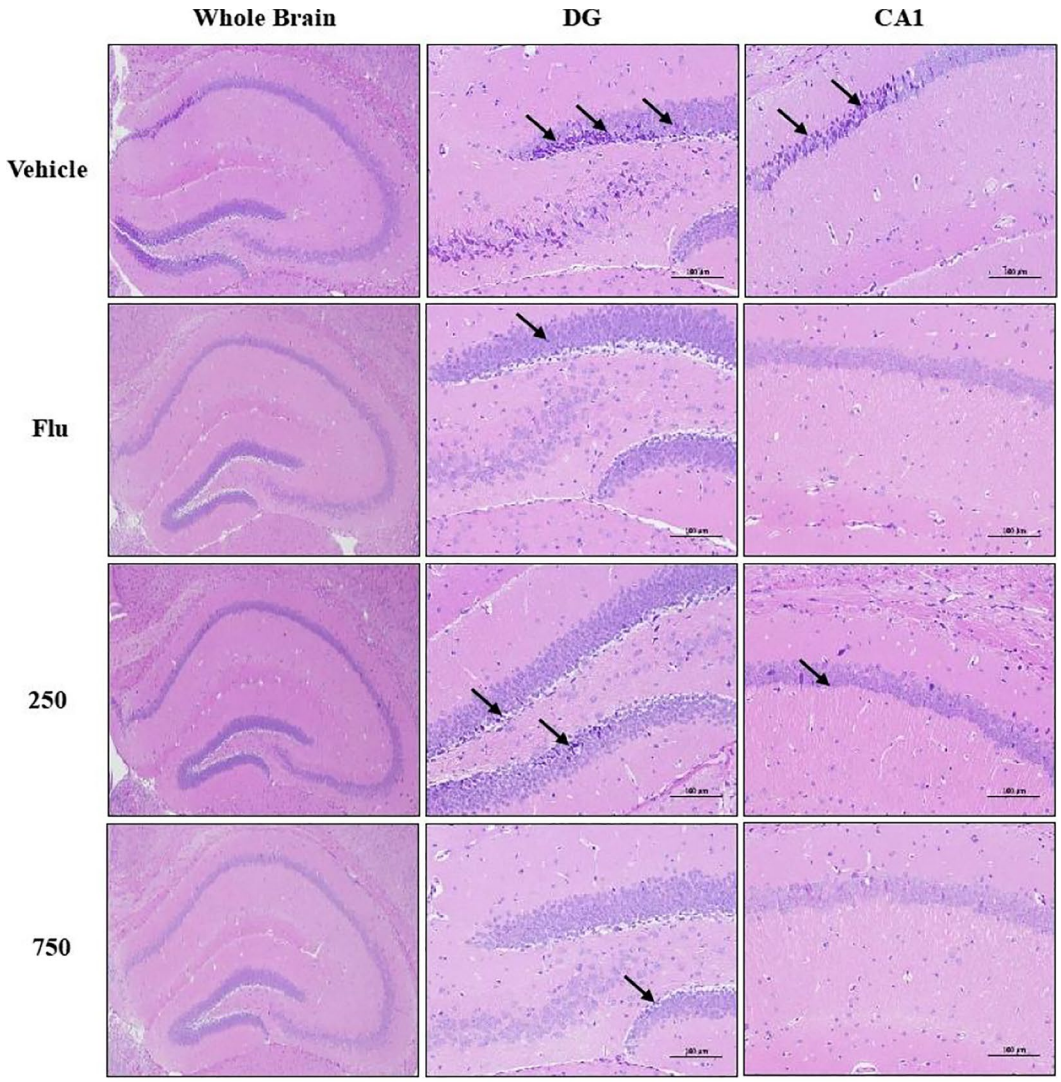

A

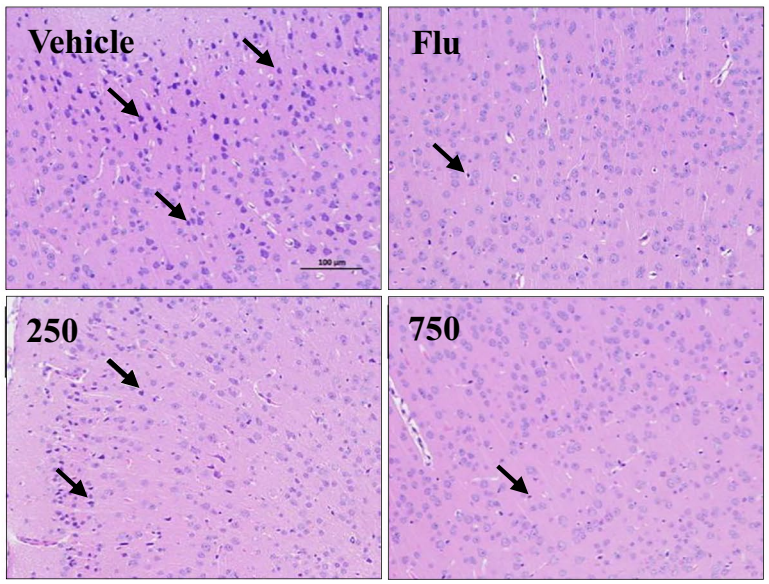

B

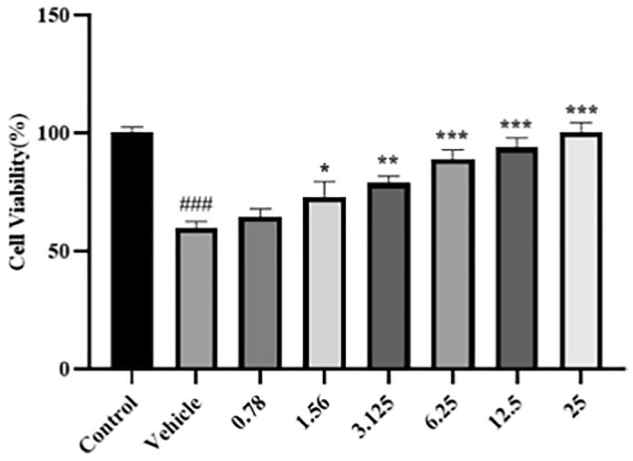

Fig. 4 The effect of cell viability by different concentration of SEO in H_2O_2-treated PC12. The values represent the mean ± SEM (n = 3 in each group), $^{*}p < 0.05$, $^{**}p < 0.01$, $^{***}p < 0.001$ compared with the Vehicle group; $^{\#\#\#}p < 0.001$ compared with the Control group

activities of different batches of SEO are presented in Table 5. The IC50 value of the ATBS radical inhibitory concentrations of the 18 batches of SEO ranged from 0.5–2.96 mg/mL. S9 showed the weakest capacity and S18 showed the strongest capacity.

GC-MS fingerprint

Total ion chromatograms were acquired for 18 batches of SEO (Fig. 8A). 19 common peaks were chosen by comparing GC-MS retention time in 18 chromatograms and are denoted in the reference fingerprint (Fig. 8B). The reference fingerprint was computed and determined by the professional software Similarity Evaluation System for Chromatographic Fingerprint of Traditional Chinese Medicine composed by the Chinese Pharmacopeia Committee (version 2009). The identification of 19 common peaks was based on matching the recorded mass spectra with the standard mass spectra in the NIST 2014 MS library and comparing their RIs with those from the literature. The identified 19 common peaks are listed in Table 6, and the relative percentage content of these peaks is listed in Table 7.

Spectrum-effect relationship

Figure 9 showed the regression coefficients calculated by PLS method between fingerprint and DPPH IC50 values (Fig. 9A), ATBS IC50 values (Fig. 9B). The regression coefficients of peaks 1, 2, 3, 4, 6, 7, 8, 9, 10, 12 and 13 were larger than zero, which means these common peaks were positively correlated with DPPH radical scavenging activity. The regression coefficients of peaks 1, 2, 3, 4, 6, 7, 8, 10 and 13 were larger than zero, which means these common peaks were positively correlated with ATBS radical scavenging activity. Combine the results of these two regressions, peaks 1 (Benzene, 1-methoxy-4-methyl-2-(1-methylethyl)-), 2 (Bicyclo[2.2.1]heptan-2-ol, 1,7,7-trimethyl-, acetate, (1S-endo)-), 3 (1,2,4-Metheno-1H-indene, octahydro-1,7a-dimethyl-5-(1-methylethyl)-, [1S-(1.alpha.,2.alpha.,3a.beta.,4.alpha.,5.alpha.,7a.beta.,8S*)]-), 4 (Ylangene), 6 (Spiro[5.5]undec-2-ene, 3,7,7-trimethyl-11-methylene-), 7 (α-Muurolene), 8 ((1R,3aS,4aS,8aS)-1,4,4,6-Tetramethyl-1,2,3,3a,4,4a,7,8-octahydrocyclopenta[1,4]cyclobuta[1,2]benzene), 10 (β-Bisabolene) and 13 ((1R,3aS,4aS,8aS)-1,4,4,6-Tetramethyl-1,2,3,3a,4,4a,7,8-octahydrocyclopenta[1,4]cyclobuta[1,2]benzene) may greatly contribute to the antioxidant activities of SEO.

Discussion

Based on the results of FST and TST, we found SEO can significantly improve the depression-like behavior in depressed mice, which indicates a promising antidepressant-like effect of SEO. Oxidative stress is caused by an imbalance between ROS production and antioxidant defenses, and these are responsible for the altered brain function associated with depression (Bhatt et al. 2020). In line with the published data, the levels of SOD, GSH, and CAT in the hippocampus, cortex, and plasma were significantly increased, and the levels of MDA in the hippocampus, cortex, and plasma were significantly decreased, which suggests an oxidative stress status in the depressed mice's brain. Besides, the histopathological examination of the hippocampus and cortex showed the brain structure has been altered. However, SEO treatment restored neuron loss and injury and attenuated the levels of oxidative stress significantly. In addition, we can draw the same conclusion in the H_2O_2-induced PC12 cells after SEO treatment by cell viability evaluation and SOD, GSH, CAT, and MDA levels detection. Therefore, these results illustrated that alleviation of oxidative stress might involve the mechanism of the antidepressant-like effect of SEO both in vitro and in vivo.

Nrf2 is known as a master regulator of redox homeostasis (Bouvier et al. 2017). During oxidative stress, Nrf2 is overactivated in the cytoplasm and translocases to the nucleus, which then leads to many antioxidant enzymes activation, such as heme-oxygenase1 (HO-1). HO-1 plays an important role in the maintenance of cell homeostasis and cell damage (Huang et al. 2021), and mediates antioxidants as a critical Nrf2-dependent transcription factor. Our data first showed that H_2O_2 did not increase the nuclear translocation of Nrf2,

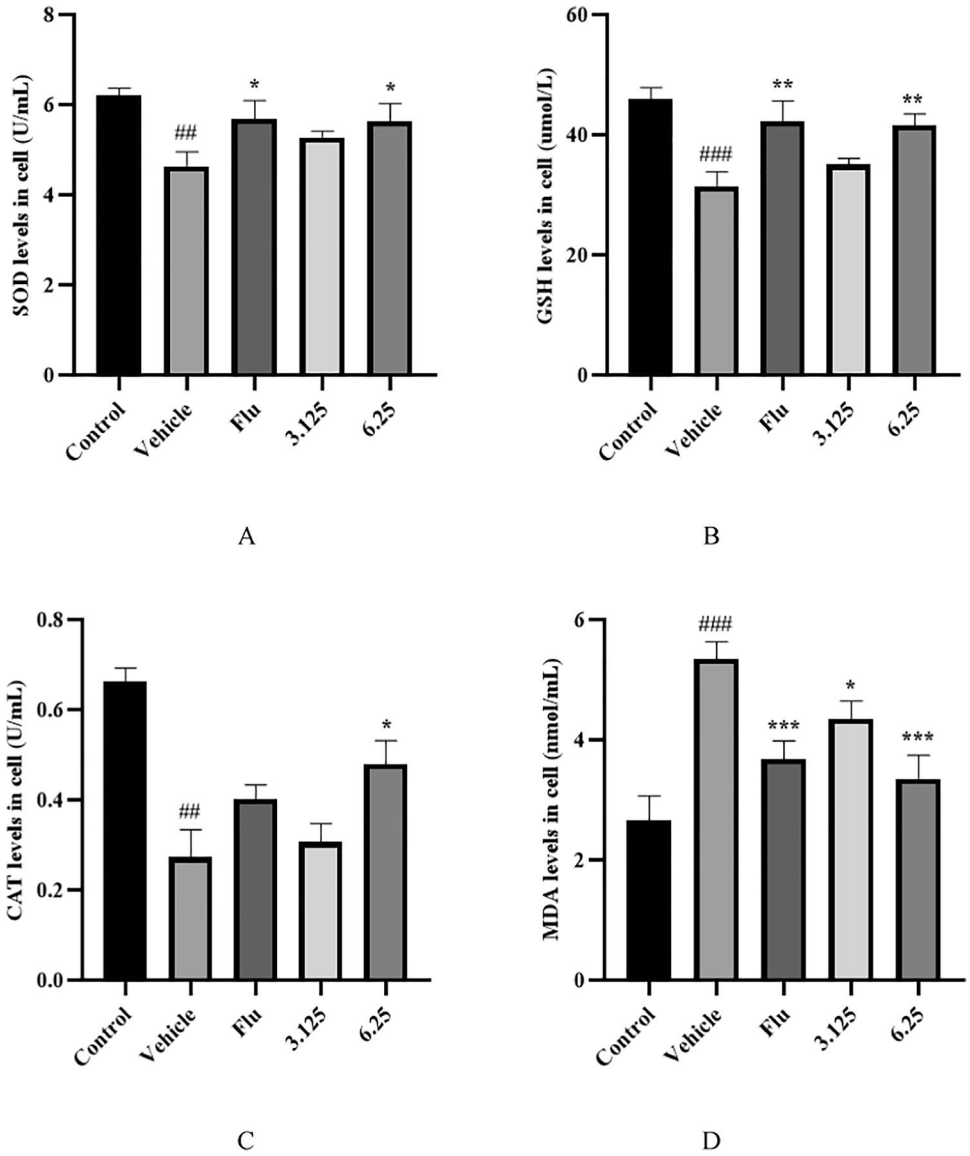

Fig. 5 The activities of SOD (**A**), GSH (**B**), CAT (**C**) and the levels of MDA (**D**) in H_2O_2-induced PC12. The values represent the mean ± SEM (n = 3 in each group), $^{*}p < 0.05$, $^{**}p < 0.01$, $^{***}p < 0.001$ compared with the Vehicle group, $^{\#\#}p < 0.01$, $^{\#\#\#}p < 0.001$ compared with the Control group

and the expressions of its downstream antioxidant enzyme HO-1 which consistent with the previous reports (Lu et al. 2022). Then, we found SEO promoted the translocations of Nrf2 to the nucleus both in the hippocampus and cortex in depressed mice, and the same results were observed in H_2O_2-induced PC12 cells as well by immunofluorescence analysis. Furthermore, SEO increased the expression of HO-1 in H_2O_2-induced PC12 cells, which indicates SEO attenuates the oxidative stress via the Nrf2/HO-1 signaling pathway regulation. PI3K/AKT/GSK3β signaling could alleviate oxidative stress by modulating the Nrf2/HO-1 pathway (Meng et al. 2021; Shin et al. 2019). PI3K/AKT is involved in the regulation of cell and physiological regeneration and pathological states (Wang et al. 2021a). GSK3β contributes to the export and degradation of Nrf2 (Liao et al. 2020). PI3K activates AKT through phosphorylation and consequently inhibits GSK3β by phosphorylation as well (Zhang et al. 2020). Consistent with published data, we found SEO could significantly increase the ratios of p-PI3K/PI3K, p-AKT/AKT, and p-GSK3β/ GSK3β in H_2O_2-induced PC12 cells. These results suggest that PI3K/AKT/GSK3β signaling promoted Nrf2/HO-1 pathway would be important in the antioxidant effect of SEO.

Based on the above results of in vivo mechanism study, we try to find out the components with good antioxidant activities in SEO. The spectrum-effect relationship analysis is to combine the chemical compositions of the fingerprint of TCM with the results of the pharmacological efficacy. The chemical fingerprint of 18 batches of SEO was established by the GC-MS method, 19 common peaks were identified

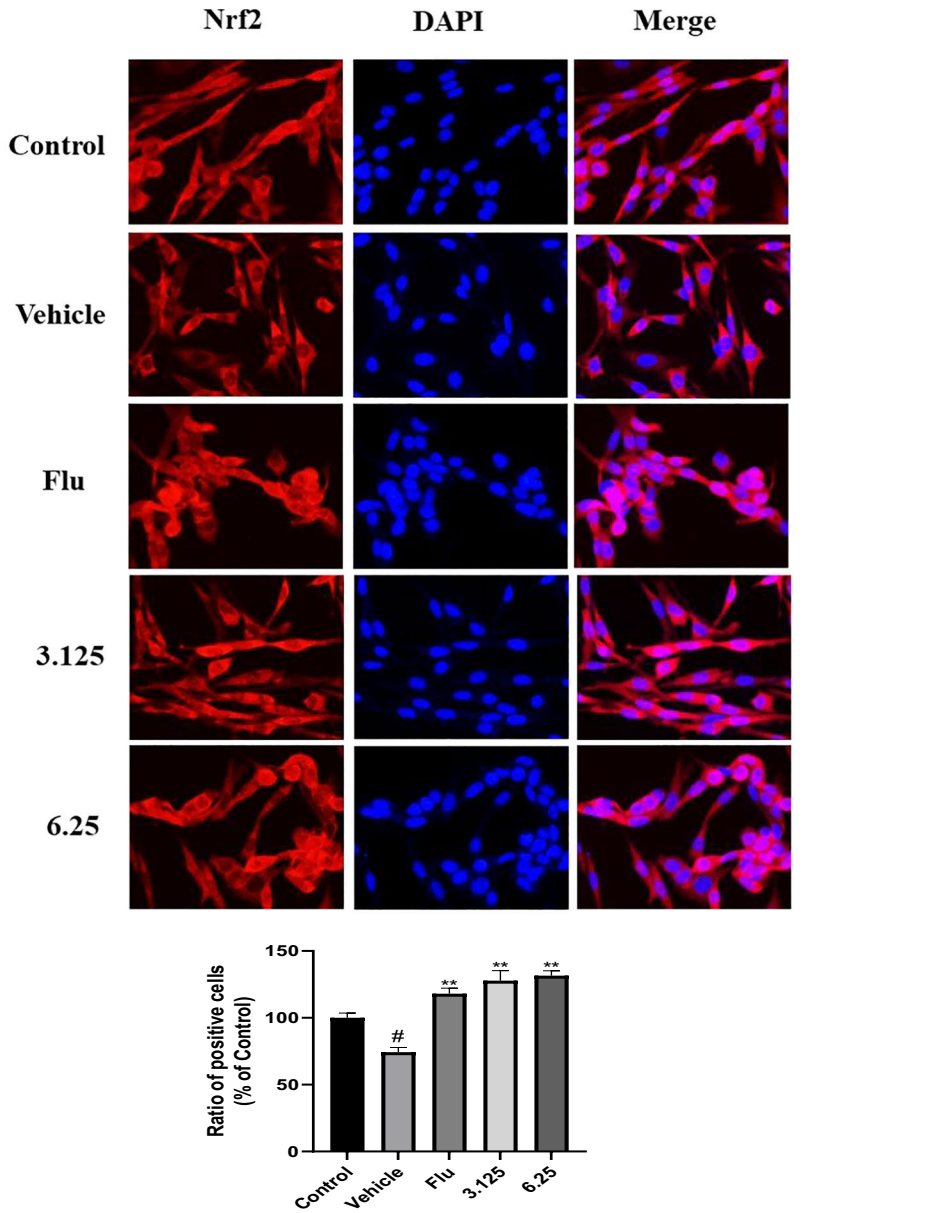
Nrf2
DAPI
Merge
Control
Vehicle
Flu
3.125
6.25
Ratio of positive cells (% of Control)
150
100
50
0
#
**
**
**
Control
Vehicle
Flu
3.125
6.25

A

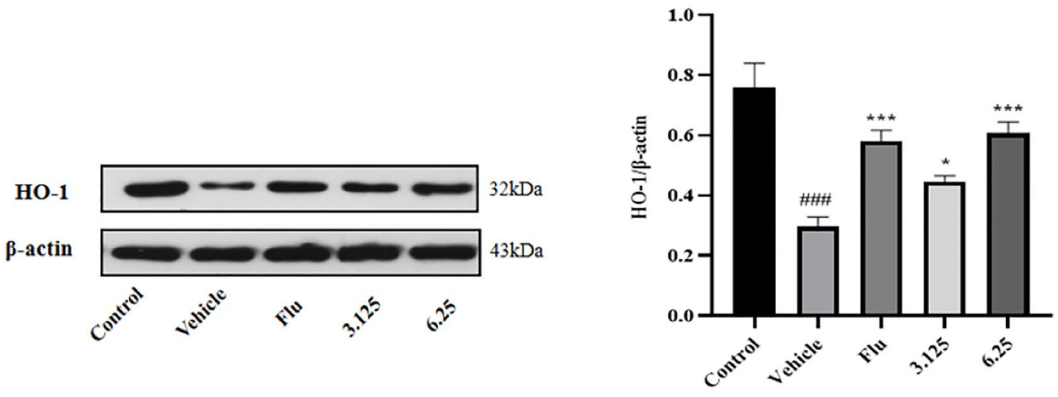
HO-1
β-actin
32kDa
43kDa
Control
Vehicle
Flu
3.125
6.25
HO-1/β-actin
1.0
0.8
0.6
0.4
0.2
0.0
###
***
*
***
Control
Vehicle
Flu
3.125
6.25

B

◀ **Fig. 6** The Effect of administration on the nuclear translocation of Nrf2 (**A**) and the protein level of HO-1 (**B**) in H_2O_2-treated PC12. The values represent the mean ± SEM (n = 3 in each group), $^{*}p < 0.05$, $^{**}p < 0.01$, $^{***}p < 0.001$ compared with the Vehicle group; $^{\#\#\#}p < 0.001$ compared with the Control group

and the relative percentage content was calculated. As shown in Tables 4 and 5, DPPH radical scavenging and ABTS values can reflect the antioxidant activity. The antioxidant activity increased with decreases of IC50 of DPPH radical scavenging and ABTS values. Combining the results of the regression coefficients plot of IC50 values of DPPH

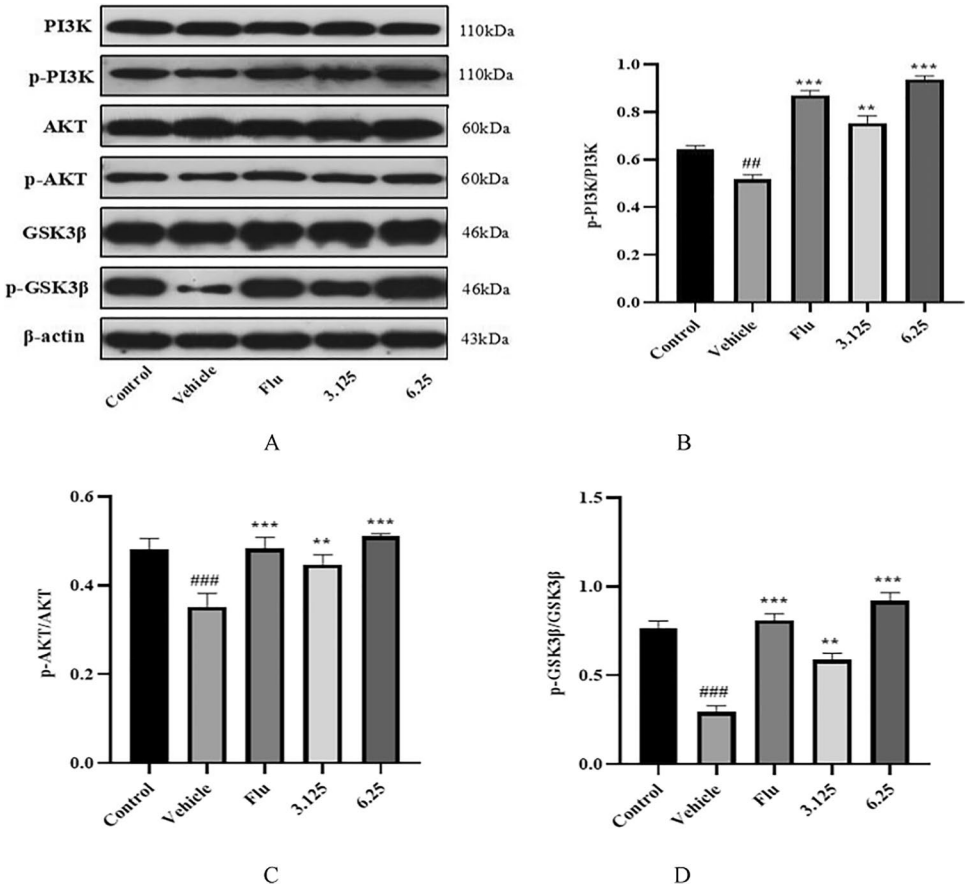

Fig. 7 The Effect of administration on PI3K, p-PI3K, AKT, p-AKT, GSK3β and p-GSK3β expression in H_2O_2-treated PC12. The expression of p-PI3K/PI3K, p-AKT/AKT and p-GSK3β/GSK3β were detected by Western Blot (**A**). (**B**), (**C**) and (**D**) graphs represented the arbitary density of blot signal. The values represent the mean ± SEM (n = 3 in each group), $^{*}p < 0.05$, $^{**}p < 0.01$, $^{***}p < 0.001$ compared with the Vehicle group; $^{\#\#\#}p < 0.001$ compared with the Control group

Table 4 IC_{50} values of DPPH assay of 18 batches of SEO

No.	IC_{50}(mg/mL)	No.	IC_{50}(mg/mL)
S1	7.35 ± 0.23[a]	S10	7.13 ± 0.08[a]
S2	7.88 ± 0.33[a]	S11	6.55 ± 0.35[a]
S3	6.32 ± 0.62[a]	S12	6.42 ± 0.07[a]
S4	7.09 ± 0.41[a]	S13	6.97 ± 0.12[a]
S5	2.99 ± 0.13[a]	S14	7.71 ± 1.14[a]
S6	8.24 ± 0.11[a]	S15	7.32 ± 0.09[a]
S7	7.15 ± 1.18[a]	S16	4.93 ± 0.13[a]
S8	6.15 ± 0.19[a]	S17	5.82 ± 0.02[a]
S9	4.57 ± 0.02[a]	S18	7.13 ± 1.33[a]

[a]Mean ± Standard deviation (SD) (n = 3)

Table 5 IC_{50} values of ABTS assay of 18 batches of SEO

No.	IC_{50}(mg/mL)	No.	IC_{50}(mg/mL)
S1	2.76 ± 0.23[a]	S10	2.17 ± 0.25[a]
S2	2.80 ± 0.15[a]	S11	2.37 ± 0.33[a]
S3	1.40 ± 0.08[a]	S12	1.21 ± 0.07[a]
S4	2.35 ± 0.30[a]	S13	1.32 ± 0.46[a]
S5	2.65 ± 0.32[a]	S14	1.62 ± 0.04[a]
S6	2.61 ± 0.07[a]	S15	1.67 ± 0.21[a]
S7	2.06 ± 0.05[a]	S16	1.26 ± 0.01[a]
S8	1.38 ± 0.13[a]	S17	1.63 ± 0.05[a]
S9	0.50 ± 0.05[a]	S18	2.96 ± 0.20[a]

[a]Mean ± Standard deviation(SD) (n = 3)

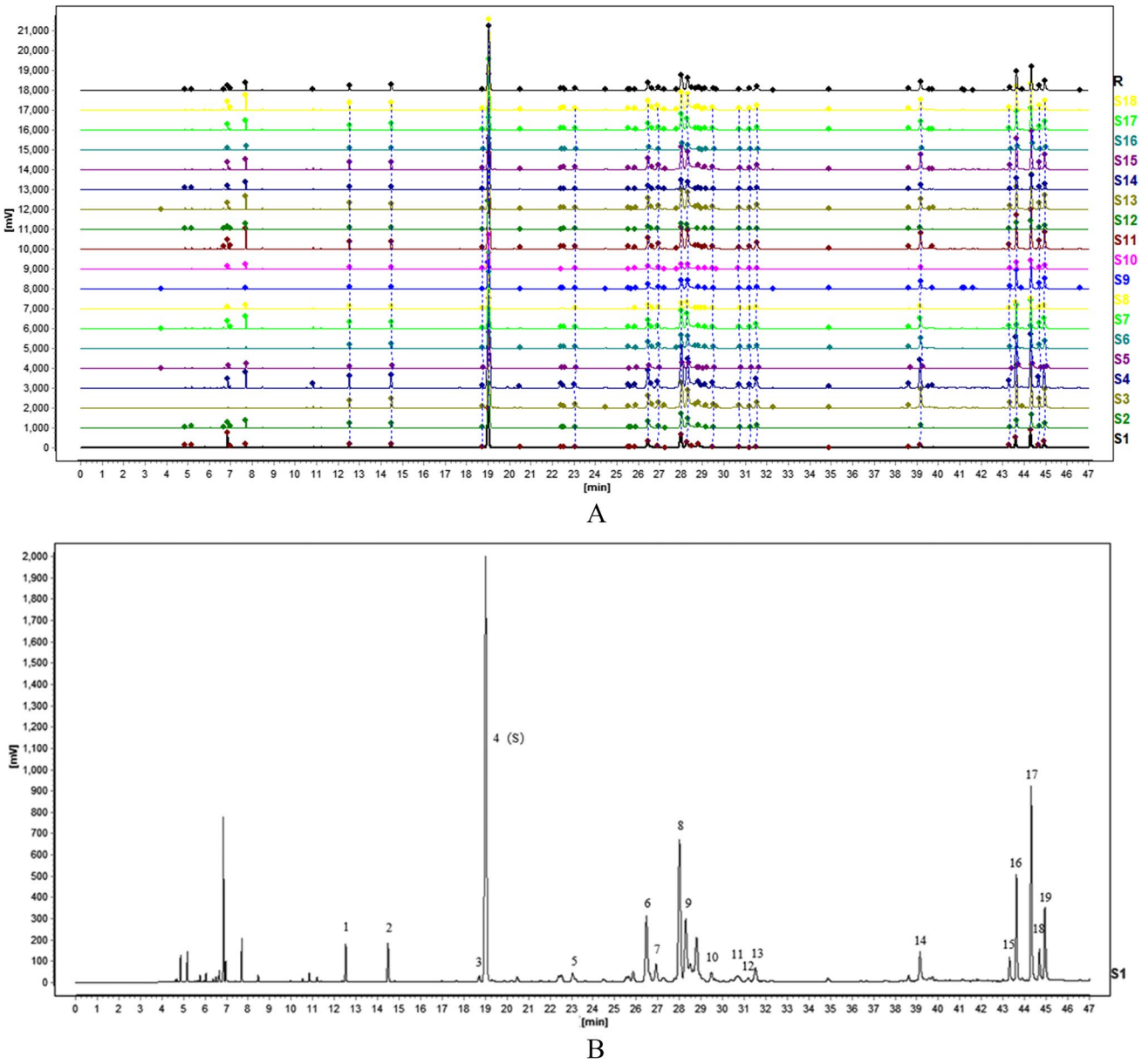

Fig. 8 GC-MS fingerprints of 18 batches of SEO (**A**), GC-MS reference fingerprint of SEO (**B**)

and ABTS, 9 peaks (peaks 1, 2, 3, 4, 6, 7, 8, 10, and 13) were identified and these peaks were positively correlated with the antioxidant effect of SEO. Previous studies reported that Ylangene (peak 4) (Liu et al. 2021a), α-Muurolene (peak 7) (Mennai et al. 2021), and β-Bisabolene (peak 10) (Obasi and Ogugua 2021) were showed promising antioxidant activity. The spectrum-effect relationship analysis results suggested that these components might be positively correlated with the antidepressant-like effect of SEO. A further study of the identified components will be performed in our future investigation, including their antioxidant effects and antidepressant-like effects.

Conclusion

In the present study, we found SEO showed a promising antidepressant-like effect in mice, and the mechanisms of this effect might be contributed to the antioxidant activities of SEO according to the results of in vitro and in vivo studies. The mechanism study indicated SEO could promote Nrf2/HO-1 pathway to improve the oxidative stress status and exert the antidepressant-like effects, and the PI3K/AKT/GSK3β signaling pathway might be involved as well. Based on the spectrum-effect relationship analysis, we found 9 peaks positively correlated with the antioxidant activity of

Table 6 The qualitative analysis result of common peaks from the fingerprint of SEO

Peak No.	Rt (min)	Compound Name	Molecular Formula	Molecular weight
1	12.53	Benzene, 1-methoxy-4-methyl-2-(1-methylethyl)-	$C_{11}H_{16}O$	164.1
2	14.48	Bicyclo[2.2.1]heptan-2-ol, 1,7,7-trimethyl-, acetate, (1S-endo)-	$C_{12}H_{20}O_2$	196.1
3	18.73	1,2,4-Metheno-1H-indene, octahydro-1,7a-dimethyl-5-(1-methylethyl)-, [1S-(1.alpha.,2.alpha.,3a.beta.,4.alpha.,5.alpha.,7a.beta.,8S*)]-	$C_{15}H_{24}$	204.2
4	19.09	Ylangene	$C_{15}H_{24}$	204.2
5	23.06	Benzene, 1,4-dimethoxy-2-methyl-5-isopropyl-	$C_{12}H_{18}O_2$	194.1
6	26.48	Spiro[5.5]undec-2-ene, 3,7,7-trimethyl-11-methylene-	$C_{15}H_{24}$	204.2
7	26.92	α-Muurolene	$C_{15}H_{24}$	204.2
8	28.09	(1R,3aS,4aS,8aS)-1,4,4,6-Tetramethyl-1,2,3,3a,4,4a,7,8-octahydrocyclopenta[1,4]cyclobuta[1,2]benzene	$C_{15}H_{24}$	204.2
9	28.35	1H-Benzocycloheptene, 2,4a,5,6,7,8-hexahydro-3,5,5,9-tetramethyl-, (R)-	$C_{15}H_{24}$	204.2
10	29.49	β-Bisabolene	$C_{15}H_{24}$	204.2
11	30.78	Naphthalene, 1,2,3,5,6,8a-hexahydro-4,7-dimethyl-1-(1-methylethyl)-, (1S-cis)-	$C_{15}H_{24}$	204.2
12	31.20	1H-Benzocycloheptene, 2,4a,5,6,7,8-hexahydro-3,5,5,9-tetramethyl-, (R)-	$C_{15}H_{24}$	204.2
13	31.54	(1R,3aS,4aS,8aS)-1,4,4,6-Tetramethyl-1,2,3,3a,4,4a,7,8-octahydrocyclopenta[1,4]cyclobuta[1,2]benzene	$C_{15}H_{24}$	204.2
14	39.18	Ylangenol	$C_{15}H_{24}O$	220.2
15	43.30	3-epi-Cedrenal	$C_{15}H_{22}O$	218.2
16	43.63	(1R,2R,4S,6S,7S,8S)-8-Isopropyl-1-methyl-3-methylenetricyclo[4.4.0.02,7]decan-4-ol	$C_{15}H_{24}O$	220.2
17	44.35	(E)-2-((8R,8aS)-8,8a-Dimethyl-3,4,6,7,8,8a-hexahydronaphthalen-2(1H)-ylidene)propanal	$C_{15}H_{22}O$	218.2
18	44.69	Bicyclo[4.1.0]heptan-2-one, 3,4,4-trimethyl-3-(3-methyl-1,3-butadienyl)-, [1.alpha.,3.alpha.(E),6.alpha.]-(.+−.)-	$C_{15}H_{22}O$	218.2
19	44.95	Ylangenal	$C_{15}H_{22}O$	218.2

Table 7 The relative percentage content of common peaks from SEO

No.	Relative area percentage																	
	S1	S2	S3	S4	S5	S6	S7	S8	S9	S10	S11	S12	S13	S14	S15	S16	S17	S18
1	1.20	1.55	0.97	1.13	1.28	0.76	1.27	1.23	0.52	–	0.99	0.90	1.03	0.82	1.16	1.11	1.04	1.18
2	1.63	2.13	1.61	1.63	2.12	1.47	1.71	1.64	0.95	1.77	1.37	1.37	1.27	1.32	1.49	1.74	1.75	1.58
3	0.36	0.43	0.49	0.43	0.53	0.53	0.48	0.51	0.25	0.62	0.47	0.49	0.43	0.50	0.50	0.49	0.49	0.50
4	28.20	33.11	31.00	26.83	40.45	36.80	33.18	41.53	19.93	40.49	29.51	36.94	29.15	36.41	33.07	38.85	33.54	33.41
5	0.40	1.02	1.12	1.03	1.01	1.00	1.08	1.05	1.01	1.10	1.01	0.96	1.02	0.74	1.05	0.86	0.96	1.00
6	5.80	6.63	4.00	4.28	4.83	3.76	4.44	4.39	5.15	5.30	4.17	3.98	4.89	3.56	4.39	4.70	3.61	4.26
7	1.30	1.56	1.79	1.39	1.54	1.87	1.70	1.57	1.67	2.01	1.42	1.57	1.18	1.69	1.79	1.57	1.68	1.83
8	11.72	12.06	8.45	10.30	8.41	7.31	8.54	6.65	7.43	7.04	7.53	8.24	8.88	8.41	8.05	10.14	9.24	8.03
9	5.74	7.13	7.31	8.96	9.67	7.99	6.90	10.60	8.96	7.89	9.00	7.42	9.96	9.01	6.17	10.11	8.46	8.99
10	0.80	0.83	1.10	1.26	0.70	1.05	1.11	1.19	0.82	0.88	1.00	0.67	0.93	0.92	0.92	0.62	0.75	1.40
11	0.92	1.15	1.64	1.30	1.04	1.46	1.31	1.02	1.57	1.45	1.39	1.11	1.28	1.25	1.32	1.05	1.27	1.29
12	0.29	1.00	0.74	0.96	0.97	0.93	1.01	0.95	1.06	0.92	0.98	0.89	1.09	0.83	0.90	0.96	0.81	0.96
13	–	–	0.33	–	–	–	–	–	0.21	–	–	–	–	–	–	–	–	–
14	1.99	2.05	4.36	5.01	2.10	4.27	3.92	2.68	4.93	2.04	4.04	2.94	3.21	3.29	4.41	–	3.51	3.24
15	1.26	0.79	1.17	1.07	0.42	0.70	1.00	0.60	1.49	0.62	0.92	0.62	0.89	0.55	1.12	0.51	0.64	0.66
16	4.93	4.18	8.12	7.12	4.82	7.86	6.87	4.58	10.00	5.70	6.75	6.04	5.66	5.83	7.07	4.30	6.20	5.85
17	8.99	7.48	8.17	7.72	5.45	7.54	8.55	6.90	15.07	7.57	7.90	8.35	8.89	7.29	9.00	6.99	6.98	6.34
18	1.57	1.24	1.80	1.64	0.75	1.38	1.66	1.17	2.77	1.35	1.78	1.44	1.72	1.31	1.91	1.19	1.26	1.29
19	3.96	3.11	3.88	3.05	2.10	2.89	3.43	2.51	5.95	3.35	3.68	3.74	3.73	2.95	3.81	3.20	3.05	2.64
Total	81.06	87.45	88.05	85.11	88.19	89.57	88.16	90.77	89.74	90.10	83.91	87.67	85.21	86.68	88.13	88.39	85.24	84.45

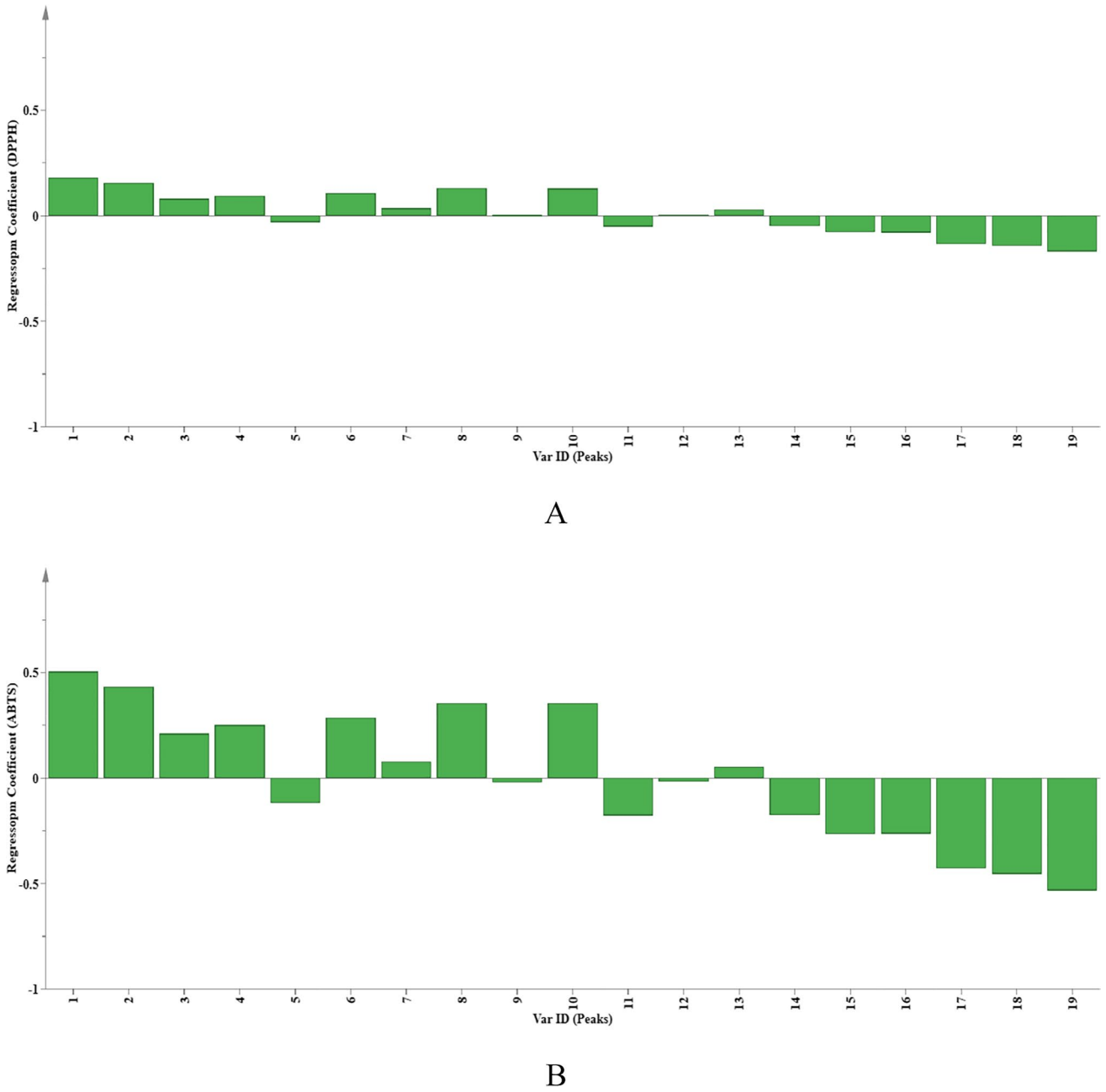

Fig. 9 The standardized regression coefficients plot of IC_{50} value of DPPH (**A**) and ABTS (**B**) radical scavenging activity of 18 batches SEO

SEO, and that is positively correlated with the antidepressant-like effects of SEO as well.

Acknowledgments This research was supported by the National Natural Science Foundation of China (No. 82173961). Key Laboratory of polysaccharide bioactivity evaluation of TCM of Liaoning Province. Liaoning Distinguished Professor Project for Ying Jia (2017). The Doctoral Scientific Research Foundation of Liaoning Province (2019-BS-233). High-level innovation and entrepreneurship team of Liaoning Province (XLYC2008029). Development Project of Qinghai Provincial Key Laboratory (2022-ZJ-Y18).

Author contributions All authors contributed to the study conception and design. Material preparation, data collection and analysis were performed by Liang Tan, Yunfang Yang, Jing Peng and Yue Zhang. The first draft of the manuscript was written by Liang Tan and Tingxu Yan and all authors commented on previous versions of the manuscript. All authors read and approved the final manuscript.

Data availability The datasets generated during and/or analysed during the current study are not publicly available due to confidential but are available from the corresponding author on reasonable request.

Declarations

Ethics approval All experiments were approved by the animal care committee of Shenyang Pharmaceutical University and performed in compliance with the national institutes of health and institutional guidelines for the humane care of animals.

Competing interests The authors have no relevant financial or non-financial interests to disclose.

References

Armario A (2021) The forced swim test: historical, conceptual and methodological considerations and its relationship with individual behavioral traits. Neurosci Biobehav Rev 128:74–86

Bhatt S, Nagappa AN, Patil CR (2020) Role of oxidative stress in depression. Drug Discov Today 25(7):1270–1276

Bouvier E, Brouillard F, Molet J, Claverie D, Cabungcal JH, Cresto N, Doligez N, Rivat C, Do KQ, Bernard C, Benoliel JJ, Becker C (2017) Nrf2-dependent persistent oxidative stress results in stress-induced vulnerability to depression. Mol Psychiatry 22(12):1701–1713

Han Y, Lee C (2009) Antidepressants reveal differential effect against 1-methyl-4-phenylpyridinium toxicity in differentiated PC12 cells. Eur J Pharmacol 604:36–44

Huang Y, Yang Y, Xu Y, Ma Q, Guo F, Zhao Y, Tao Y, Li M, Guo J (2021) Nrf2/HO-1 Axis regulates the angiogenesis of gastric Cancer via targeting VEGF. Cancer Manag Res 13:3155–3169

Lee J-H, Lee Y-Y, Lee J, Jang Y-J, Jang H-W (2021) Chemical composition, antioxidant, and anti-inflammatory activity of essential oil from Omija (*Schisandra chinensis* (Turcz.) Baill.) produced by supercritical fluid extraction using CO_2. Foods 10:1619. https://doi.org/10.3390/foods10071619

Liao S, Wu J, Liu R, Wang S, Luo J, Yang Y, Qin Y, Li T, Zheng X, Song J, Zhao X, Xiao C, Zhang Y, Bian L, Jia P, Bai Y, Zheng X (2020) A novel compound DBZ ameliorates neuroinflammation in LPS-stimulated microglia and ischemic stroke rats: role of Akt(Ser473)/GSK3β(Ser9)-mediated Nrf2 activation. Redox Biol 36:101644

Liu C, Zhang S, Zhang J, Liang Q, Li D (2021) Chemical composition and antioxidant activity of essential oil from berries of Schisandra chinensis (Turcz.) Baill. Nat Prod Res 26(23):2199–2203

Liu L, Zheng B, Wang Z (2021b) Protective effects of the knockdown of lncRNA AK139328 against oxygen glucose deprivation/reoxygenation-induced injury in PC12 cells. Mol Med Rep 24(3):621. https://doi.org/10.3892/mmr.2021.12260

Lu C, Day C, Kuo C, Wang T, Ho T, Lai P, Chen R, Yao C, Viswanadha V, Kuo W, Huang C (2022) Calycosin alleviates H O -induced astrocyte injury by restricting oxidative stress through the Akt/Nrf2/HO-1 signaling pathway. Environ Toxicol 37(4):858–867

Meng M, Zhang L, Ai D, Wu H, Peng W (2021) β-Asarone ameliorates β-amyloid-induced neurotoxicity in PC12 cells by activating P13K/Akt/Nrf2 signaling pathway. Front Pharmacol 12:659955

Mennai I, Lamera E, Slougui N, Benaicha B, Gasmi S, Samai Z, Rahmounia N, Bensouici C, Pinto DCGA (2021) Chemical composition and antioxidant, antiparasitic, cytotoxicity and antimicrobial potential of the Algerian Limonium oleifolium mill. Essential oil and organic extracts. Chem Biodiversity 18(9):e2100278. https://doi.org/10.1002/cbdv.202100278

Obasi D, Ogugua V (2021) GC-MS analysis, pH and antioxidant effect of Ruzu herbal bitters on alloxan-induced diabetic rats. Biochem Biophys Rep 27:101057

Ong ES, Oh CLY, Tan JCW, Foo SY, Leo CH (2021) Pressurized hot water extraction of okra seeds reveals antioxidant, antidiabetic and vasoprotective activities. Plants (Basel, Switzerland) 10(8):1645. https://doi.org/10.3390/plants10081645

Park S, Lee Y, Yang H, Song G (2021) Fluoxetine potentiates phagocytosis and autophagy in microglia. Front Pharmacol 12:770610

Shin JH, Kim KM, Jeong JU, Shin JM, Kang JH, Bang K, Kim J-H (2019) Nrf2-Heme Oxygenase-1 attenuates high-glucose-induced epithelial-to-mesenchymal transition of renal tubule cells by inhibiting ROS-mediated PI3K/Akt/GSK-3β signaling. J Diabetes Res 2019:2510105–2510105

Wang D, Liu J, Jiang H (2021a) Triclosan regulates the Nrf2/HO-1 pathway through the PI3K/Akt/JNK signaling cascade to induce oxidative damage in neurons. Environ Toxicol 36(9):1953–1964. https://doi.org/10.1002/tox.23315

Wang Y, Chen Y, Jia Y, Xue Z, Chen Z, Zhang M, Panichayupakaranant P, Yang S, Chen H (2021b) Chrysophyllum cainito. L alleviates diabetic and complications by playing antioxidant, antiglycation, hypoglycemic roles and the chemical profile analysis. J Ethnopharmacol 281:114569. https://doi.org/10.1016/j.jep.2021.114569

Yan T, Wang N, Liu B, Wu B, Xiao F, He B, Jia Y (2021) Schisandra chinensis ameliorates depressive-like behaviors by regulating microbiota-gut-brain axis via its anti-inflammation activity. Phytother Res: PTR 35(1):289–296

Zhang X, Chen J, Yang J, Shi Y (2018) UPLC-MS/MS analysis for antioxidant components of Lycii Fructus based on spectrum-effect relationship. Talanta 180:389–395

Zhang J, Ding C, Zhang S, Xu Y (2020) Neuroprotective effects of astaxanthin against oxygen and glucose deprivation damage via the PI3K/Akt/GSK3β/Nrf2 signalling pathway in vitro. J Cell Mol Med 24(16):8977–8985

Zhang L, Tang M, Xie X, Zhao Q, Hu N, He H, Liu G, Huang S, Peng C, Xiao Y, You Z (2021a) Ginsenoside Rb1 induces a pro-neurogenic microglial phenotype via PPARγ activation in male mice exposed to chronic mild stress. J Neuroinflammation 18(1):171

Zhang Y, Long Y, Yu S, Li D, Yang M, Guan Y, Zhang D, Wan J, Liu S, Shi A, Li N, Peng W (2021b) Natural volatile oils derived from herbal medicines: a promising therapy way for treating depressive disorder. Pharmacol Res 164:105376

Zhang Z, Yang Y, Liu X, Qin Z, Li S, Bai L, Li J (2021c) The protective effect of aspirin eugenol Ester on oxidative stress to PC12 cells stimulated with HO through regulating PI3K/Akt signal pathway. Oxidative Med Cell Longev 2021:5527475